Journal of Hydrology 587 (2020) 124947

Contents lists available at ScienceDirect

Journal of Hydrology

journal homepage: www.elsevier.com/locate/jhydrol

Research papers

Spring discharge and thermal regime of a groundwater dependent ecosystem in an arid karst environment

Todd G. Caldwell[a,c,*], Brad D. Wolaver[a], Tara Bongiovanni[a], Jon P. Pierre[a], Sarah Robertson[b], Charles Abolt[a], Bridget R. Scanlon[a]

[a] Bureau of Economic Geology, Jackson School of Geosciences, The University of Texas at Austin, Austin, TX, United States
[b] Texas Parks and Wildlife Department, San Marcos, TX, United States
[c] Nevada Water Science Center, U.S. Geological Survey, Carson City, NV, United States

ARTICLE INFO

Keywords:
Groundwater dependent ecosystems
Karst hydrology
Springs
Refugia
Climate change
Fisheries

ABSTRACT

In semi-arid regions, groundwater-dependent ecosystems rely on stable hydro-thermal regimes where refugia have supported aquatic biota for millennia. In karst systems, springs provide consistent flows and stenothermal conditions that buffer extremes. Our objective was to assess the impacts of spring discharge on instream temperatures, using the pristine Devils River in Texas as a case study, where climate change and groundwater development threaten to reduce spring flows and aquatic habitats of protected species (Devils River minnow and Texas hornshell mussel). Instream temperatures and discharge were monitored for three years above and below the Finegan Spring complex. These time series were extended back 30 years using temperature data from North American Land Data Assimilation System (NLDAS) land surface models. Monitoring data revealed that springs contributed ~40% of total river discharge. Spring temperatures were consistently 22.6 ± 0.3 °C providing thermal refugia to 200 m of river—cooling the streamflow in summer and warming it in winter, with a noted stratification overturning each winter. High correlations between NLDAS air and soil temperatures and instream temperatures allowed the water temperature record to be extended over 30 years. While air and soil temperatures increased 0.35 °C and 0.30 °C per decade, spring inputs from karst aquifer buffer downstream temperature increases to 0.12 °C per decade. Furthermore, spring discharge reduced the duration of extreme thermal habitat thresholds by 50–70%. A similar approach could be applied to other groundwater dependent ecosystems with sparse temperature data. The results underscore the importance of spring discharge in maintaining heterogeneous aquatic habitats in karst terrain.

1. Introduction

Groundwater discharge to streams generally plays a critical role in stabilizing flows, mediating water temperatures, and supporting riverine ecosystems (Constantz, 1998; Briggs et al., 2013; Burns et al., 2017). The thermal regimes of riverine ecosystems are fundamentally critical to fish and other aquatic organisms whose physiologic processes are dictated by the temperature of the ambient environment (Atkinson, 1994; Poole and Berman, 2001; Colinet et al., 2015). When stream temperatures exceed critical thresholds, reproduction and biological functions of aquatic species can be impaired or mortality can occur. The sensitivity of biota to stream temperature has motivated many studies to investigate the impact of climate change (Mohseni and Stefan, 1999) and establish physical thresholds for events influencing the survivability of threatened species (Capra et al., 1995; Castelli et al., 2012; Briggs et al., 2013; Davis et al., 2013).

For cold-water systems, many studies have highlighted the importance of shade from riparian vegetation buffering stream temperatures (Albertson et al., 2018; Wondzell et al., 2019) because solar radiation is the dominant component of the river heat budget (Webb and Zhang, 1997). Advective heat fluxes from groundwater and rainfall, and sensible heat transfer between air and water are the next most important inputs to this heat budget (Webb and Zhang, 1997). Decoupled from local rainfall, habitats supported by groundwater are generally buffered from extreme temperatures (Davis et al., 2013). Groundwater dependent ecosystems (GDE) include wetlands, lakes, rivers, and springs that rely on groundwater inputs to support both terrestrial and subterranean ecosystems (Brown et al., 2011). Many are under threat from the compound effects of groundwater exploitation and changing climate, particularly in arid and semi-arid regions globally and the

* Corresponding author at: Nevada Water Science Center, U.S. Geological Survey, Carson City, NV, United States.
E-mail address: tcaldwell@usgs.gov (T.G. Caldwell).

https://doi.org/10.1016/j.jhydrol.2020.124947

Available online 20 April 2020
0022-1694/ Published by Elsevier B.V.

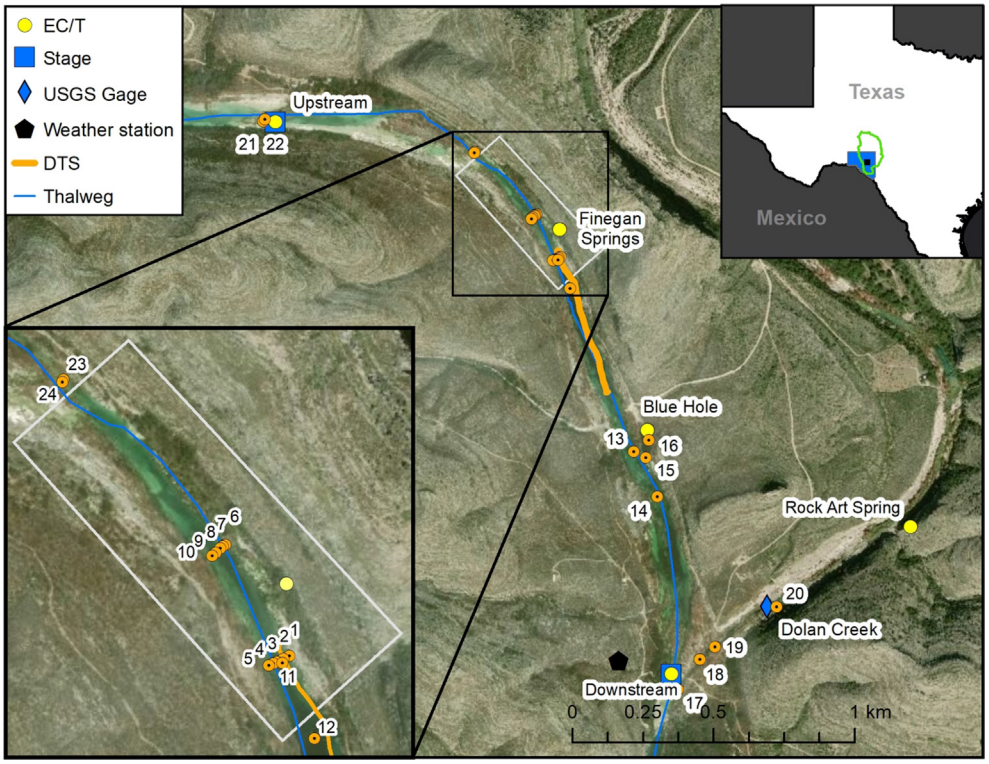

Fig. 1. Study area and design for monitoring locations for lateral T_w transects (#1–5, #6–10) below Finegan Springs, longitudinal transects, DTS cable location, and stage/discharge measurement locations (Upstream and Downstream). The Dolan Creek (USGS gage 08449100) longitudinal transect (#17–20) begins in the perennial reach of Dolan Creek beginning at Rock Art Spring. Inset includes the Devils River watershed (HUC6) in Val Verde County, TX.

western U.S. (Rohde et al., 2017).

Springs represent particularly unique GDE, occurring at the groundwater and land–atmosphere-water interface (Springer and Stevens, 2009). Springs tend to be focused areas of aquifer discharge where the groundwater table is at or above the land surface elevation. Spring-fed GDE in drylands are generally recharged by a combination of relict groundwater with long regional flow paths and localized flow paths that more quickly respond to mesoscale precipitation events (Robertson et al., 2019b). Understanding groundwater dynamics and their effects on spring discharge and thermal refugia are essential to developing effective instream flow recommendations for GDE (Hardy, 1998; Acreman and Dunbar, 2004). The importance of groundwater discharge in providing thermal refugia within the context of climate change is increasingly being recognized (Kurylyk et al., 2014; Snyder et al., 2015; Hausner et al., 2016; Kaandorp et al., 2019). Furthermore, groundwater is a critical component of instream flows, providing stable water levels, temperatures, and nutrients for riverine ecosystems (Power et al., 1999). In critical habitats of Texas, instream flows are required to meet a sound ecological environment, including a suite of measurable, basin-specific ecological indicators (National Research Council, 2005).

In karst systems, such as the Edwards-Trinity (plateau) aquifer in Texas, discharge from springs has created evolutionary refugia supporting endemic fishes and aquatic biota (Craig et al., 2016). Semi-arid spring complexes that support GDE commonly have stenothermal biota (i.e. biota that are adapted to a narrow temperature range) (Mott Lacroix et al., 2017). The hydrological regime of lotic (fast flowing water) ecosystems can further constrain fish assemblages (Poff and Allan, 1995). The native species in riverine systems possess life history traits that enable them to survive within certain ranges of environmental conditions, such as current velocity, depth, water temperature, and oxygen content (Allan and Castillo, 2007). The thermal and hydrological regimes of such GDE are poorly understood particularly in karst aquifer systems where spring discharge predominantly supports perennial surface waters and riverine habitats.

The interaction between instream temperatures, streamflow, and groundwater exchange has received little attention in gaining reaches of karst terrain. Heat has been used as a surrogate for groundwater flux input in many hydrological settings (Anderson, 2005) and there are various approaches to quantifying groundwater discharge to surface waters, including heat flux methods from temperature profiles (Constantz, 1998; Constantz et al., 2016), fiber optic distributed temperature sensing (DTS) (Selker et al., 2006; Briggs et al., 2012; Hausner et al., 2012; Briggs et al., 2013; Briggs and Hare, 2018), and remotely sensed methods (Huntington et al., 2016; Mundy et al., 2017; Pai et al., 2017; Abolt et al., 2018). Moreover, instream temperatures from internally powered and recorded sensors (Johnson et al., 2005; Isaak and Horan, 2013) or externally controlled thermistors/thermocouples provide temporal temperature data at discrete locations and depths (Wagner et al., 2006). Quantification of thermal refugia may require a combination of these techniques (Hare et al., 2015; Dzara et al., 2019). Regardless of the method, there are inherent difficulties and challenges to sustaining field measurements over prolonged times in remote areas (Burt and McDonnell, 2015).

The objective of this study was to evaluate linkages between the karst aquifer-spring-stream systems to assess their influence on thermal buffering of groundwater-dependent riverine habitats, using the Devils River in Texas as a case study. The following questions were addressed:

1. What are key factors influencing instream temperatures proximal and distal to spring discharge?
2. What long-term trends exist in riverine thermal regimes upstream and downstream of spring complexes?
3. What are the critical thermal and/or hydrological regimes that should trigger water management intervention?

This study presents several unique field and modeling approaches to characterize surface–groundwater interactions within an arid karst GDE. Remote watersheds are inherently difficult to monitor, let alone assess long-term trends or controls. We developed novel techniques to predict instream temperatures from hydroclimatic data and then used long-term weather forcing data from the NLDAS land surface models to construct extended (30-year) water temperature records. Using these reconstructed records, decadal-scale temperature trends were

developed for habitat temperature-duration thresholds by quantifying the frequency and duration of continuous events above specified temperatures (Castelli et al., 2012).

2. Materials and methods

2.1. Study area

The study site was a section of the perennial reach of the semi-arid, groundwater-dependent Devils River within the Devils River State Natural Area (SNA) and The Nature Conservancy (TNC) Dolan Falls Preserve (Fig. 1; Figs. S1–S3, in Supporting Information) in Val Verde County, Texas. The study site focused on the Finegan Springs complex and the confluence of the Devils River and Dolan Creek, ~60 km north of the city of Del Rio. This reach is considered an "Ecologically Significant Stream Segment" nominee due to its relatively intact ecosystem and high species diversity (El-Hage and Moulton, 2001). The uniqueness of the aquatic ecosystem is in large part due to perennial water in a relatively arid climate with average annual precipitation of 50 cm and mean annual temperature of 18–20 °C (PRISM, 2018). The watershed provides a range of terrestrial and aquatic habitats attributed to its location at the convergence of the Chihuahuan Desert, Edwards Plateau, and Southern Texas Plains ecoregions (TWPD, 2012).

The Devils River is a major tributary to the Rio Grande, terminating in Amistad Reservoir which began impounding flows from the Rio Grande, Devils, and Pecos rivers in 1968 (Fig. S7). Now, it is jointly managed by the United States and Mexico through the International Boundary and Water Commission. The Devils River is 145 km long but only the lower 95 km are perennial, primarily due to consistent groundwater inputs from numerous springs (Green et al., 2014; Abolt et al., 2018). These springs are particularly clear with consistent flow and temperatures providing thermal stability some distance downstream. As these spring-runs become exposed to ambient air temperatures, the thermal stability decreases downstream (Hubbs, 1995; Springer and Stevens, 2009). The perennial reach of the Devils River began near Juno, TX until 1970 when groundwater development for irrigation lowered the regional water table (Barker and Bush, 1994). Today, Pecan Springs ~10 km downstream of Juno marks the start of the perennial reach, which is now the upper range of the Devils River minnow. The Devils River, perhaps the least developed and most scenic river in Texas, is one of the last strongholds for multiple species of regionally endemic freshwater fishes and mussels. The watershed provides a diversity of habitat types supporting numerous aquatic and terrestrial species, including several regional endemics classified as threatened or endangered at both the state and federal levels (Robertson et al., 2019a).

The Devils River, and its tributary Dolan Creek, are habitat to five Texas state-threatened aquatic species, including the Proserpine Shiner (*Cyprinella proserpina*), Conchos Pupfish (*Cyprinodon eximius*), Rio Grande Darter (*Etheostoma grahami*), Devils River Minnow (*Dionda diaboli*), and Texas hornshell (*Popenaias popeii*) (El-Hage and Moulton, 2001). *D. diaboli*, also listed as federally threatened, has a narrow distribution (Hubbs and Brown, 1956) and has faced a number of threats including the 1950's drought across the Midwest and Texas, the construction of Amistad reservoir which eliminated suitable habitat in part of its range, and anthropogenic alteration of tributaries in Mexico (USFWS, 2005). Since inundation in 1968, Goodenough Spring, once one of the very large springs of Texas, has had a consistent discharge of 2.03 $m^3\ s^{-1}$ (Kamps et al., 2009). Groundwater discharge from springs at the Finegan and Blue Hole spring complex support important habitat of *D. diaboli* and the heterogeneous structure of riverine fishes (Kollaus and Bonner, 2012). Development of groundwater that potentially changes spring discharge is a specific threat to this habitat. The same is true for Texas Hornshell, a regional endemic that is currently listed as federally endangered and, like other Unionids, is thought to be sensitive to extreme warm water temperatures, especially in early life stages.

Land use in the Devils River Watershed comprises shrub/scrub (96%), grasslands/herbaceous (2.2%), deciduous/evergreen forest (1.2%), and minimally developed land (0.2%; Fig. S5) (MRLC, 2018). Developed land historically included conventional oil and gas production, primarily from the Lower Ellenburger Group. Horizontal wells for hydraulic fracturing have recently expanded to the upper Devils River basin and surrounding area (Fig. S6). Today, the Devils River is threatened by large inter-basin water transfer projects to arid west Texas and by encroaching development of wind energy. Motivated by the threat of proposed groundwater extraction, the primary driving factor of this research was to assess the influence of spring discharge on instream temperatures relative to critical habitats.

2.2. Hydrology of the Devils River watershed

The Devils River has incised into the Edwards Plateau creating steep canyons and ephemeral drainages inset into the relatively flat carbonaceous bedrock, which gently dips to the southeast. Unlike the adjacent Pecos River watershed, the Devils River is entirely underlain by low-permeability limestone, resulting in a nearly synchronous response of its tributaries during extreme rainfall events (Kochel et al., 1982). The underlying karstic Edwards-Trinity Aquifer (Abbott, 1975) is present throughout the study area and discharges at springs and seeps into the Devils River which maintains base flows during dry seasons. The potentiometric surface is a subdued expression of surface topography and water flows from higher elevations on the Edwards Plateau to Amistad Reservoir and the Rio Grande (Fig. S7). Within the study area, the aquifer comprises two formations of the lower Cretaceous Edwards Group: the unconfined Segovia and the underlying Fort Terrett formations.

Recharge in karst terrain such as this occurs primarily through episodic flows in drainage channels, such as Dolan Creek, the Dry Devils River, and the upper Devils River. Groundwater flows from north to south along preferential flow paths parallel to the Devils River (Green et al., 2014). Natural spring discharge occurs as rheocrene or hillslope spring types (following the nomenclature of Springer and Stevens (2009)) where drainage channels have eroded down since development of the distal Balcones Fault system in the Early Miocene and intersected the water table (Abbott, 1975). In our study area, springs discharge at the Segovia-Fort Terrett contact, where limestone dissolution along this horizon (possibly the Kirschberg evaporite zone) allows preferential groundwater flow to discharge, forming the Finegan-Blue Hole-Dolan spring complex, which essentially doubles the river discharge downstream.

2.3. River stage, discharge, spring contribution, and groundwater levels

River stage was measured at locations upstream and downstream of the Finegan Spring complex (Fig. 1) by installing absolute pressure transducers (9 m range, ± 0.1% full scale, Rugged TROLL 100, In-Situ, Fort Collins, CO) in a mount affixed to the limestone stream bottom. Stage and temperature were sampled every 15 min. River stage was corrected using barometric pressure data (Section 2.5) recorded on site. Instantaneous discharge (Q) was periodically measured at both locations using an acoustic Doppler velocimeter (FlowTracker, SonTek, San Diego, CA) to develop a stage-discharge relationship (Rantz, 1982). Our rating curve used instantaneous discharge measurements and a 24-hour mean (centered around the time of the discharge measurement) stage measurement as

$$Q = p(G - e)^N \quad (1)$$

where G is recorded stage height at the gage, e is gauge height of effective zero-flow, p is discharge when (G-e) is 1, and N is the slope of the rating curve. For the downstream location, e was set to zero. For the upstream location, graphical methods were used to determine any changes in e by observing a parallel shift in the rating curve. The spring

complex discharge was calculated as the difference between downstream and upstream discharge.

Groundwater levels were measured at two existing wells using absolute pressure loggers (11 m range, ± 0.05% full scale, In-Situ Level Troll 500, Fort Collins, CO). The shallow well (depth 76.5 m) is located ~300 m south of Dolan Creek ~20 m above an active channel (Fig. S7). The deep well (depth 203 m) is located on a high plateau, ~120 m above the channel and ~5 km east of Dolan Creek. Groundwater levels were sampled at 1-hour intervals.

2.4. Instream water temperatures (T_w)

Water temperatures (T_w) and specific conductance were measured in the orifice of three springs (Fig. 1, Finegan, Blue Hole, and Rock Art) with an accuracy of ± 0.1 °C and ± 5 µs cm^{-1}, respectively (U24, Onset Corp., Bourne, MA). T_w was measured along two lateral and two longitudinal transects below the spring complex using Tidbit temperature loggers (± 0.2 °C, Onset Corp., Bourne, MA). Both lateral transects had five sensors housed in a protective vinyl cap affixed with a concrete anchor to a rock on the bottom of the stream spanning the channel from one bank into the thalweg and to the other side (Fig. 1, #1–10). Longitudinal T_w measurements were collected down the Devils River and from Blue Hole (#14–16), and down Dolan Creek (Fig. 1, #17–20) to the confluence. For longitudinal transects, loggers were attached to the downstream side of boulders in the stream channel (Isaak and Horan, 2013).

Four fiber optic DTS surveys of varying duration 10/20/15 (26 h), 02/24/16 (40 h), 9/27/16 (14 h), and 2/8/17 (25 h) were conducted when spring and stream temperatures were expected to have the largest separation (i.e. summer and winter). For each survey, the DTS was positioned in the thalweg below the Finegan Springs complex using two fiber optic cables: ~400 m upstream and the other ~600 m downstream (Fig. 1). The DTS (N4386B, Agilent Technologies, Böblingen, Germany) sends discrete laser pulses down a continuous, looped 2 km optical fiber (BRUsens Temperature 85C mobile, 4.6 mm, Brugg Kabel AG, Switzerland), where it scatters and returns to the detector. The incidental Ramen and Brillouin backscattering allow us to estimate stream temperature along the entire length of the cable (Selker et al., 2006). The Agilent DTS allows a 1 m spatial sampling with 0.1 °C resolution. Double-ended DTS measurements were collected every 90 s and averaged every 6-minutes at 1-m intervals. Differential attenuation along the fiber optic cable was directly measured using double-ended measurement configuration in the instrument software. The dynamic offset of the DTS was corrected using controlled water baths with ~25 m of cable coiled in each. Two water baths, one ambient and one ice, were constantly mixed using an aquarium bubbler during data collection. Water temperatures in each bath were monitored using platinum resistance thermometers and used to correct raw temperature trace files (van de Giesen et al., 2012). Corrected temperature vectors upstream and downstream were concatenated and averaged over the collection period to produce a continuous longitudinal mean (and standard deviation) of 1 m stream temperatures.

2.5. Meteorological data

We established a weather station (Fig. 1) to monitor air temperature (T_a) and relative humidity (HC2S3, Rotronic Instrument Corp., Hauppauge, NY), soil temperature (T_s) (P107, Campbell Scientific, Logan, UT) at 10 cm depth, short-wave solar radiation (Model 8–48, Eppley Laboratory, Inc., Newport, RI), wind speed and direction (Model 03002, R.M. Young Co., Traverse City, MI), and precipitation (TE525, Texas Electronics, Dallas, TX). A self-contained barometric pressure sensor (BaroTROLL, In-Situ, Fort Collin, CO) was used for post-processing non-vented pressure transducers. Each sensor was sampled every 5 s and averaged every 30 min. Daily potential evapotranspiration (PET) was calculated using a modified Penman equation based on maximum and minimum T_a and relative humidity, mean wind speed, and solar radiation.

3. Thermal modeling and data analysis

3.1. Instream temperature modeling

Linear correlations between environmental covariates (e.g. T_a or T_s) and T_w are used to obtain an empirical model of the climatic influence on instream temperatures (Mohseni and Stefan, 1999). The general formulae are:

$$T_w(t) = A + BT_a(t) or T_w(t) = A + BT_s(t) \quad (2)$$

where water temperature (T_w) is linearly dependent on either air temperature (T_a) and soil temperature (T_s) (°C) averaged over some specified time interval (t). Least-squares linear regression was used to determine the constant (A) and slope (B) of this relationship, which generally proves to be linear above freezing and below 30 °C. The slope of this relationship, B, represents the thermal sensitivity of T_w at a given site to either T_a or T_s (Kelleher et al., 2012). Thermal sensitivity tends to be lower when groundwater inputs are higher (Beaufort et al., 2019). For shorter time intervals ($t < 1$ day), time lags can be incorporated (Stefan and Preudhomme, 1993). Here, Eq. (2) was used to model each instream location at hourly and daily (mean, maximum, and minimum) intervals. Statistical significance ($p < 0.05$) was determined from a parametric Student t-test and model performance by means of the coefficient of determination (R^2) and root mean square error (RMSE).

We also developed a more complex, multiple linear regressive (*mlr*) model that incorporated both the daily mean stage at our lower gage (G_L) and daily mean solar radiation (R_s)

$$T_w(t) = C_0 + C_1T_a(t) + C_2T_s(t) + C_3G_L + C_4R_S \quad (3)$$

where the additive combination of these five parameters (C_0 to C_4) is determined again by least-squares regression and G_L was only used because its more stable limestone channel.

Lastly, a stepwise (*sw*) linear regression was developed, which iteratively adds and removes predictor variables (T_a, T_s, G_L, and R_s) as the p-value of the F statistic either improves or degrades model performance. The final model may include interactions, products, and power functions of these predictors. Thus, the *sw* model is indicative of our lowest possible RMSE that empirically predicts T_w given all other measurement (predictor) variables; however, it was explicitly trained for the entire study period and is not useful outside of these bounds; it is essentially our "best" achievable fit over our data collection period for comparison to other models.

3.2. Long-term trend analysis

As with most field-based studies, we were only able to monitor environmental data over a relatively short, ~3-year period (Jan. 2016–Dec. 2018). Sensor failures, data loss, and other inconsistencies that come with field data collection in remote locations were common. However, data collection could be supplemented if there were consistent and statistically significant relationships with other long-term climate reanalysis products. The NLDAS data archive consists of a primary forcing data set from 1979 to present which is used to drive four independent land surface models (LSM) over the conterminous United States (Mitchell et al., 2004). The primary forcing data set consists of 11 hourly climatic variables, including precipitation, T_a, long- and short-wave radiation, and absolute humidity at 2 m (Xia et al., 2012). These data are gridded at 1/8° (~12 km) spatial resolution and available at http://disc.sci.gsfc.nasa.gov/hydrology/data-holdings.

The Devils River Hydrologic Unit Codes (HUC) for HUC_8, HUC_{10}, and HUC_{12} was used to extract-by-mask T_a and R_s from the NLDAS data, and T_s from the Noah LSM. Note, the HUC number is inversely proportional to watershed area (Fig. S8) and a HUC_8, HUC_{10} and HUC_{12}

references 23, 7 and 3 NLDAS cells, respectively. Each cell was averaged into an hourly value, then calculated the daily mean, max and minimum T_a and T_s, and daily mean R_s for each HUC size.

Next, like the *mlr* $T_w(T_a, T_s, R_s)$ model, we replaced the observed weather data with NLDAS T_a, T_s, and R_s and derived optimal coefficients over the study period. Finally, the *mlr* was applied to a 30-year NLDAS record (1988–2018) to model T_w at each instream location, creating daily time series of mean, maximum, and minimum T_w for trend analysis. We assumed that the *mlr* developed was applicable over the past 30-years and that spring flow, spring temperature, and vegetation shading, etc., were relatively consistent. This assumption seems reasonable given the pristine conditions within the watershed, but it remains intrinsic to our trend analysis.

For each location, the 30-year daily mean, maximum, and minimum were calculated for each thermal model. These data were binned incrementally by day of year (DOY) in intervals (i = 1:30 days) to assess temporal autocorrelation (i.e. verify time-independent data). Once the minimum i was determined (i.e. where autocorrelation is insignificant at a given i-lag), an annual climatology was calculated by averaging each DOY bin over the 30-year record. The temperature anomaly (T_{anom}) was then determined by subtracting this climatology from each predicted T_w averaged over i. Serial correlation was reduced ($R < 0.2$) when $i > 5$d (Fig. S9; Ljung-Box Q-test, $p < 0.05$ for lags of 1i, 5i and even 10i). Thus, the data were binned weekly (i = 7) and monthly (i = 30); the latter is preferred in the climate literature. However, critical above-threshold temperatures are generally less than ~30 days (Section 3.3), so we attempted to preserve enough data to maintain persistent summer extremes, while also minimizing statistical issues in the trend analysis. In essence, the T_{anom} removes covariance and seasonal signal allowing the long-term, linear trend to be calculated with least-squares linear regression and statistical significance ($p < 0.05$) from a parametric Student t-test, which assumes the data are normally distributed and the residuals have a zero mean with constant variance. However, a non-parametric Mann-Kendall test was performed which determines the monotonic significance ($p < 0.05$) of any trend that may be linear or non-linear and makes no assumption about the residuals.

3.3. Thermal habitat thresholds

The thermal tolerance of fishes reflects a combination of biotic and abiotic factors that include acclimation temperature and thermal history (Chung, 2001). The frequency and duration of thermal events was determined from time series analysis by uniform continuous above-threshold (UCAT) analysis (Castelli et al., 2012). Originally applied to environmental flow conditions under a given threshold (Capra et al., 1995; Parasiewicz, 2008), UCAT analysis essentially counts events over a given temperature threshold, computing each event duration and taking its ratio to total length of time series (e.g., see Fig. S10). These ratios are shown as the cumulative frequency versus the cumulative duration; the y-axis on a UCAT plot indicates event duration, while the x-axis indicates cumulative time during which an event of that duration or longer occurred. We repeated this procedure in 1 °C increments for daily maximum T_w at the upstream and downstream locations using data between June 1 and September 30 from the 30-year modeled time series mentioned previously. Inflection or breakpoints between catastrophic and critical threshold days were determined using piece-wise linear regression. These points demarcate rapid changes in frequency of continuous durations where persistent or rare conditions may affect one generation, while catastrophic events are longer duration and can impact multiple generations (Castelli et al., 2012).

4. Results

Results are presented first over the 3-year monitoring period from 1 January 2016 to 30 December 2018 and modeled over 30 years (1989–2018). The former is termed the “study period” and the latter “long-term”. Similarly, we use “spring complex” as the contribution of spring discharge which includes multiple sources (e.g. Finegan and Blue Hole complexes), all of which are bound by the upstream and downstream monitoring locations.

4.1. Meteorological conditions over the study period

Maximum daily air temperatures (T_a) exceeded 40 °C each year in late summer while minimum T_a dropped below freezing most winter months, with January 2017 being particularly cold (Table S1). Late summer and early fall tend to have more rainfall, often exceeding 100 mm. Measured annual precipitation totaled 739 mm in 2016 and 560 mm in 2017. The thirty year normal (1981–2010) mean annual precipitation is 517 mm at Finegan Springs (PRISM, 2018), making both years slightly wetter than normal. Precipitation was generally less than PET demand given the aridity index (AI = PPT/PET) of 0.44 in 2016 and 0.34 in 2017, which classifies the Devils River observations as semi-arid ($0.2 < AI < 0.5$). However, the monthly AI was ≥ 1 during four months of the study period: October 2015, August 2016, December 2016, and May 2017.

4.2. River and spring discharge

Discharge measurements (Table 1) above the spring complex (upstream) ranged from 0.32 to 4.27 $m^3\ s^{-1}$ (11 to 151 $ft^3\ s^{-1}$), while below (downstream) ranged from 1.09 to 5.56 $m^3\ s^{-1}$ (38 to 196 $ft^3\ s^{-1}$). The residual is spring discharge, which ranged from 0.77 to

Table 1
Measured discharges above and below Finegan Springs sorted from low to high percentage of total downstream discharge.

Date	Upstream discharge		Downstream discharge		Spring discharge		
	$ft^3\ s^{-1}$	$m^3\ s^{-1}$	$ft^3\ s^{-1}$	$m^3\ s^{-1}$	$ft^3\ s^{-1}$	$m^3\ s^{-1}$	% Total downstream discharge
5-Oct-17	151	4.27	196	5.56	45	1.29	23%
2-Feb-19	146	4.13	209	5.92	63	1.78	30%
4-Oct-16	88	2.49	134	3.80	46	1.32	35%
14-Nov-17	58	1.66	92	2.61	34	0.95	36%
27-Sep-16	103	2.91	176	5.00	73	2.08	42%
9-May-17	47	1.32	82	2.33	35*	0.99*	43%
13-Jun-16	45*	1.28*	82*	2.31*	36	1.03	44%*
20-Mar-18	29	0.82	54	1.52	25	0.71	47%
9-Feb-17	41	1.16	79	2.24	38	1.08	48%
25-Feb-16	29	0.82	59	1.67	30	0.84	51%
20-Oct-15	16	0.45	44	1.24	28	0.79	63%
28-Sep-15	11	0.32	38	1.09	27	0.77	71%

*Median value.

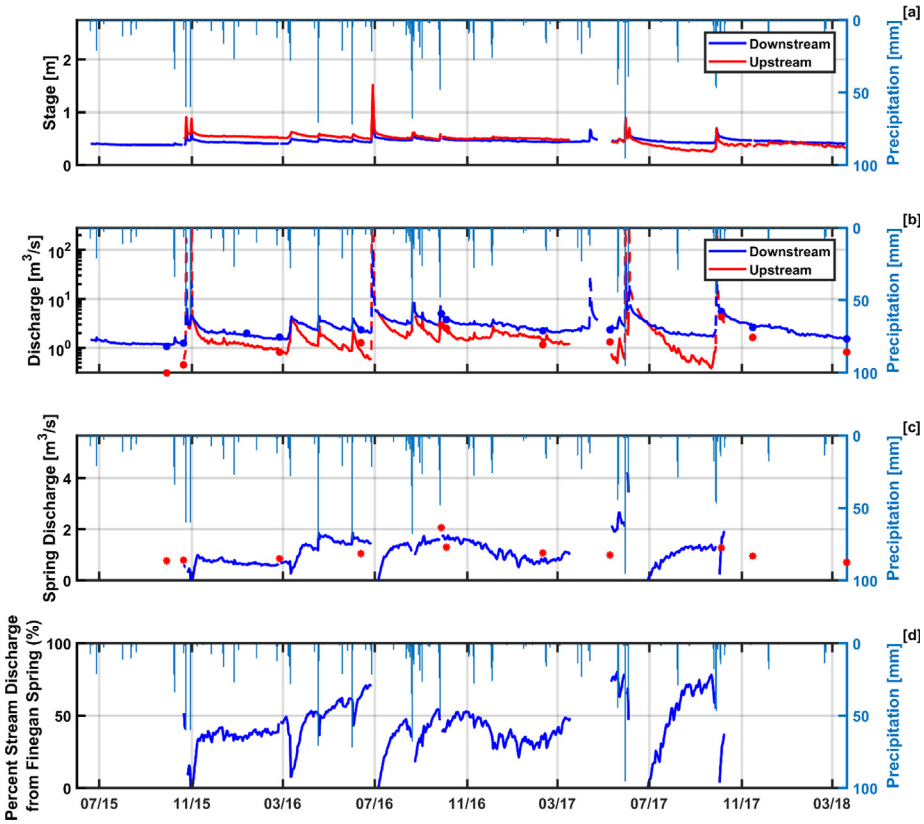

Fig. 2. Devils River [a] stage, [b] calculated discharge at upstream and downstream locations, [c] Finegan Spring complex discharge by difference, and [d] percentage of spring flow contribution to total flow. Red circles denote discharge measurements (dates and discharge rates are provided in Table 1). Dashed discharge lines [b] indicate periods beyond the derived stage-discharge rating curve. (For interpretation of the references to colour in this figure legend, the reader is referred to the web version of this article.)

1.29 $m^3\ s^{-1}$ or 71% to 23% of total river discharge. The median measured discharges upstream, spring, and downstream were 1.28, 0.99 and 2.31 $m^3\ s^{-1}$, respectively. Relative stages during discharge measurements ranged from 0.50 to 0.64 m at the upstream location producing a discharge rating curve with an RMSE of 0.51 $m^3\ s^{-1}$, an R^2 of 0.88, and two changes in effective gage height (Fig. S11a), while stage at the downstream location ranged from 0.40 to 0.54 m, producing a rating curve with an RMSE of 0.39 $m^3\ s^{-1}$, an R^2 of 0.95 and no adjustment in effective gage height (Fig. S11b). Continuous monitoring of stage showed dynamic and short-term peaks reaching ~1.8 m and quickly returning to 0.4 m (Fig. 2a). Downstream discharge was consistently greater than upstream discharge, indicating a gaining reach (Fig. 2b) from spring inputs (Fig. 2c). Following *Rantz* (1982), the spring discharge record was constrained to periods when the observed stages were within the bounds of the rating curve and determined the average Finegan Springs complex contribution was 43% to total river discharge (Fig. 2d). Flow duration analysis over these periods indicates that median discharges upstream, spring complex, and downstream were 2.11, 1.53, and 2.41 $m^3\ s^{-1}$, respectively.

4.3. Spring, groundwater, and river temperatures

Water temperatures (T_w) at discrete springs, including Finegan Spring (FS), Blue Hole (BH), and Rock Art (RA) were relatively constant, with minimal seasonal fluctuations (± 0.5 °C) and deviations that were correlated positively with larger precipitation events in summer and negatively in winter (Fig. 3a). Site #16 (Fig. 1) was in a pool just below Blue Hole and had substantially larger diurnal variability. Specific conductance (not shown) at these springs was also relatively constant (~500 μS cm^{-1}) and decreased to ~200 μS cm^{-1} following major precipitation events as fresher water entered the catchment.

The static groundwater elevations of the shallow (440 masl) and deep (436 masl) wells were > 30 m above the river elevation of 404 masl at Dolan Creek (USGS Gauge 08449100). This potentiometric difference provided the hydraulic head needed to maintain consistent spring discharge. During high discharge events in Dolan Creek, groundwater levels in the shallow well increased rapidly by ~10 m. The deep well maintained a constant level until the borehole partially collapsed in March 2018. Despite the high dynamic range of head in the shallow well, T_w remained stable at 22.6 °C; T_w in the deep well was 22.9 °C (Fig. 3b).

River T_w (Fig. 3c) revealed the importance of spring discharge when comparing the difference between downstream and upstream temperatures (ΔT; Fig. 3d). Downstream T_w was nearly ~4 °C warmer in the winter and up to 3 °C cooler in the summer. Spring discharge, which was about half of the downstream discharge and originated from groundwater with a nearly constant T_w of ~ 23 °C thus providing thermal buffering for this GDE.

4.4. Instream water temperatures

Instream T_w from the longitudinal transect (Fig. S12a) spans 2.8 km. Upstream T_w amplitudes were attenuated by spring inputs along the entire length of this transect. The lateral upper and lower transects began on the eastern bank (spring side) and progressed to the far bank. The middle positions (7, 8, 9 and 2, 4) reached ~23 °C in summer with little diurnal variability (Fig. S12b and c). In winter, stream temperatures were highly correlated to each other and much more dynamic, regardless of lateral position. The sensors were placed on the streambed under water depths ranging from 0.5 m on or near the banks to 2 m in the thalweg. In summer, cooler spring waters descended to the thalweg and warmer more dynamic river waters remained near the surface. In winter, the upstream input was colder and dynamically linked to T_a and the warmer spring water essentially floated on top (Abolt et al., 2018).

The cumulative distribution functions (F(x)) of measured T_w at the springs indicate nearly constant temperatures of 23 °C (Fig. 4a) while upstream has a wider distribution both laterally with more extreme T_w

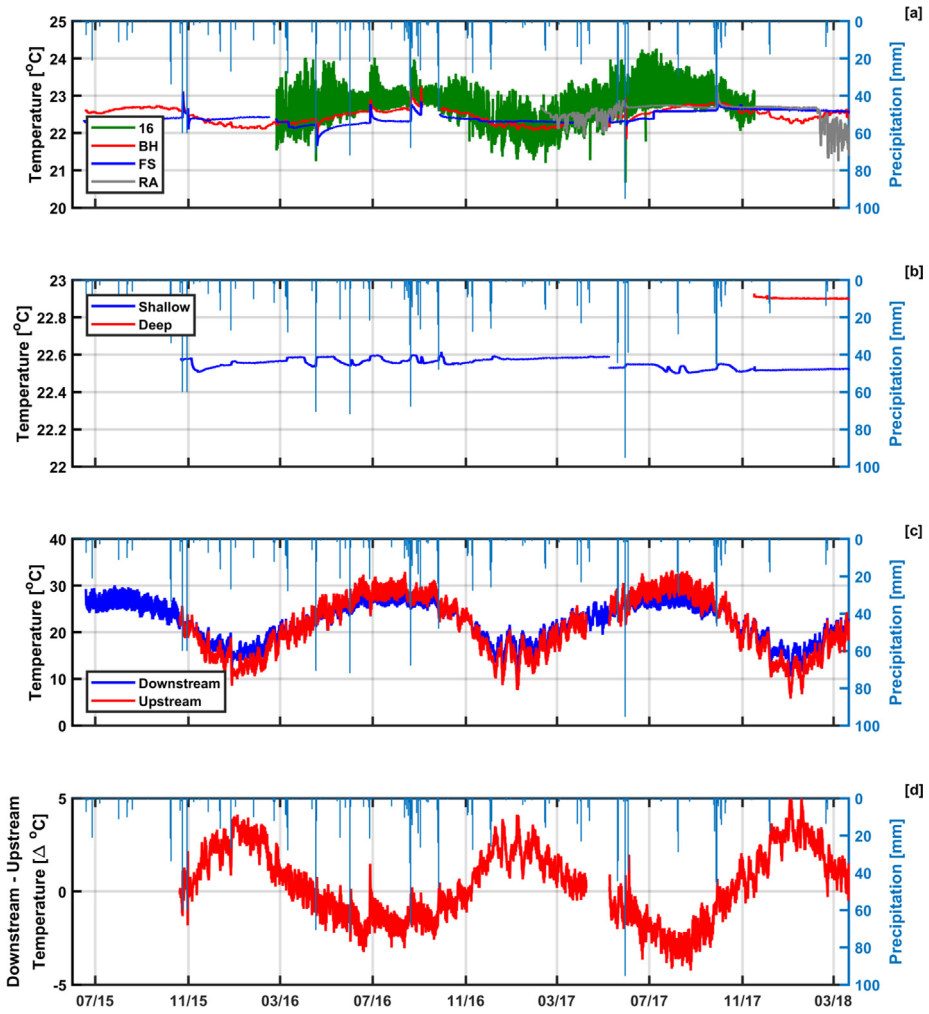

Fig. 3. Water temperature at [a] Finegan Springs complex including Blue Hole (16 and BH), Finegan Spring (FS) and Rock Art Spring (RA), [b] groundwater, [c] instream at upstream and downstream locations and [d] the differential between downstream and upstream. (For interpretation of the references to colour in this figure legend, the reader is referred to the web version of this article.)

variations on the far bank (Fig. 1, #10) than the downstream lateral transect. The F(x) for both T_a and T_s (Fig. 4d) were essentially buffered by inputs from the springs as shown longitudinally in Fig. 4e. Finally, the short transect down Dolan Creek ending in the lower Devils River (Fig. 1, #20 – 17) had consistently cooler T_w upstream (Fig. 4f).

Four DTS surveys were conducted under two different thermal regimes: warm (20 October 2015 and 28 September 2016) when river water was generally warmer than spring waters (~23 °C) and cold (2 February 2014 and 8 February 2017) when river waters (~15 °C) were cooler than springs. We attempted to reposition the DTS cable in the thalweg either resting on the limestone or vegetated stream bottom. The upstream end (distance ~400 m) extended just below the spring complex ending (distance ~ 600 m) upstream of BH spring (see Fig. 1). Data collection times varied but all were sampled over the course of at least one diurnal cycle with the goal to define spring inputs, which should be areas of low variance over a 24-hr period.

In both warm situations, a strikingly low variance was found along the entire 1 km of cable (Fig. 5a and c). Regardless of position or time of day, the DTS temperatures were essential 23 °C and equivalent to spring waters. Conversely, during cold surveys (Fig. 5b and d), DTS temperatures were cooler upstream (fiber section 200–400 m) then warmed to 17 °C below Finegan and Blue Hole, but the variance of ± 3 °C. Similarly, in 2017's cold survey (Fig. 5d), a warming downstream 100 m was observed with cooler temperatures upstream and high variance along the entire cable length.

During our final cold survey, thermal infrared temperature (TIR) data was collected using an unmanned aerial vehicle (Abolt et al., 2018). TIR captured the skin temperature of the water. Clearly, cooler upstream river water mixed with two warmer spring inputs downstream. The DTS distance of 400 m upstream is in these cooler river waters. The warmer spring water inputs essentially float atop the river water with only modest mixing. Considering that the DTS thalweg temperatures show high diurnal variance (i.e. river water), this would imply instream stratification. Conversely, the warm surveys show little diurnal variation, implying the spring waters remain in the thalweg and do not fully mix within this reach, although it certainly mixes below Dolan Falls.

This stratification is notable at the upper transect (Fig. 6a) just below the spring complex when the spring-side bottom temperatures (Fig. 1, #6) remain constant at 23 °C until the first large flood pulse arrives on 11 November 2015. This event mixes water on the stream surface lowering T_w below 23 °C. This surface water temperature signal remains on the river bottom all winter, as noted in the 2016 cold DTS survey (20160224; Fig. 5b). The first warm survey (20151020) was synchronous with a period when all the instream temperatures converged. The lower transect (Fig. 6b) is ~150 m downstream of the upper transect. The bottom T_w records are warmer until a modest cold front arrives a few days prior to our second warm survey (20160928) which homogenized T_w of the DTS measurement period at the lower transect. Unfortunately, the upper transect sensors malfunctioned

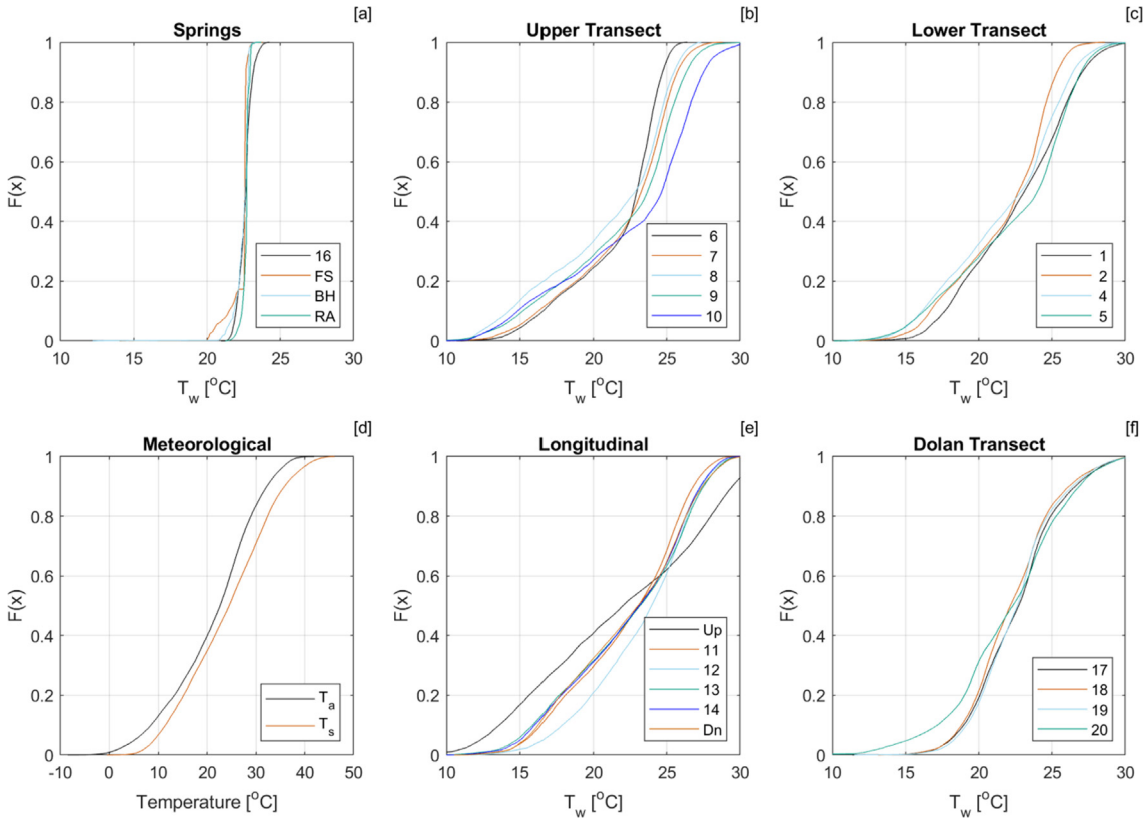

Fig. 4. Cumulative distribution of measured hourly instream temperatures of [a] springs, lateral transects, [b] upstream transect and [c] downstream transect, [d] air temperature (T_a) and soil temperature (T_s), and longitudinal transects of the [e] Devils River and [f] Dolan Creek.

during this DTS survey. However, it seems plausible that thermal stratification in the Devils River is common below the spring complex where laminar flow exists (Fig. S2) until Dolan Falls fully mixes these waters (Fig. S3).

4.5. Empirical modeling of instream water temperature and long-term trends

Qualitatively, T_w has strong seasonality that is overprinted with random diurnal variability mimicking T_a in all non-spring locations. Generally, T_w lagged T_a (T_s also lagged T_a). Correlations with T_w were

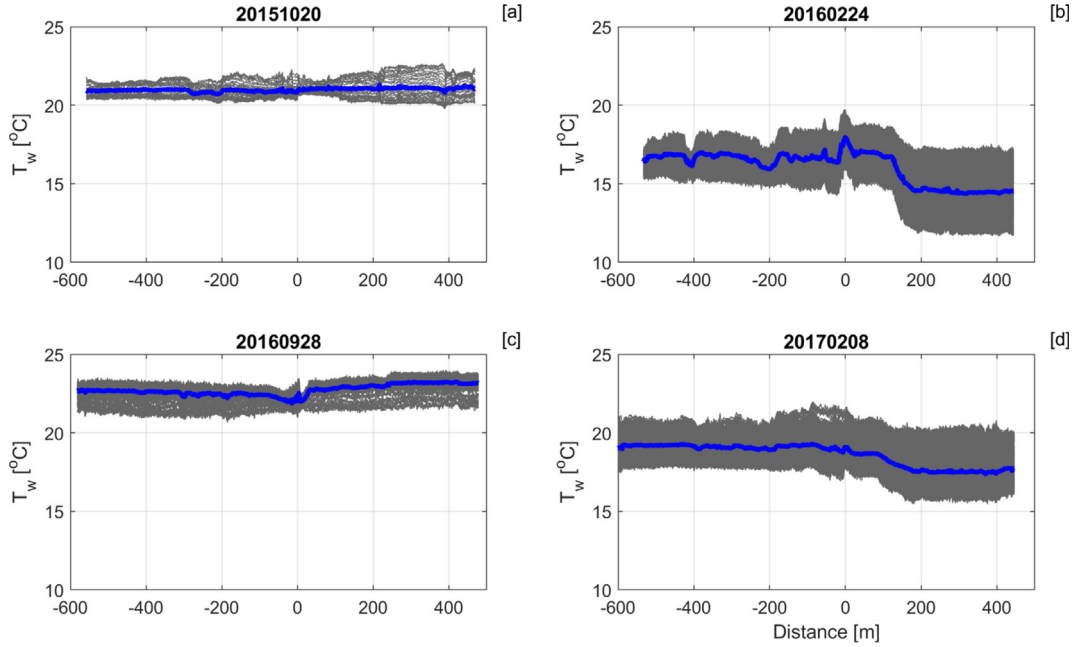

Fig. 5. Fiber optic DTS measurements for [a] October 2015, [b] February 2016, [c] September 2016, and [d] February 2017. Gray lines indicate 6-minute measurements aggregated into mean (blue) for the measurement period. The origin distance (0 m) indicates the junction of the ~ 400 m upstream and ~ -600 m downstream cable. (For interpretation of the references to colour in this figure legend, the reader is referred to the web version of this article.)

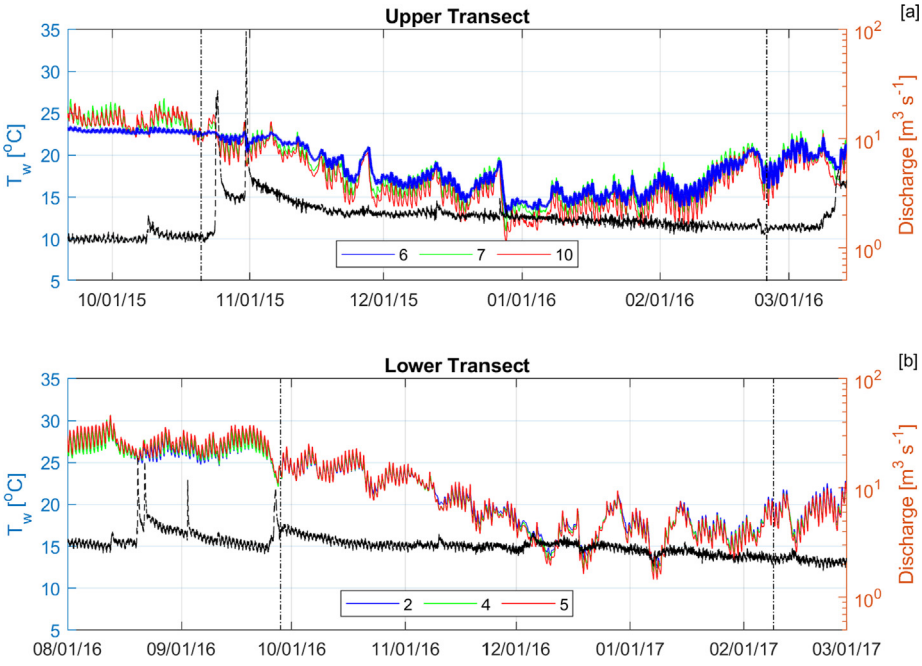

Fig. 6. Continuous discharge (black line) at Dolan Crossing and instream T_w along the (a) upper lateral transect in 2015–2016 and (b) lower lateral transects in 2016–2017. Dashed vertical lines denote DTS collection times. Each fall T_w in the thalweg near spring discharge (#2 and #6) retain spring temperatures until significant flow events mix waters and the thalwegs become homogeneous with upstream surfaces waters that are considerably cooler and vary diurnally.

particularly high ($R > 0.8$) for both T_a and T_s but at nearly all locations it was higher with T_s. Using hourly data, a lagged correlation matrix was implemented from −24 to +24 h preserving the highest correlation coefficient (R) and its lag period (Fig. S13). The lag between T_a and T_w at nearly all instream locations was only 2–3 h and between 0 to −1 lag hours for T_s. Note, negative lags indicate earlier arrival at the independent location than the dependent location. Correlation between instream sensors was particularly high for all locations, except for the Dolan Transect (Fig. 1, #17–20). Spring locations were excluded here due to low thermal sensitivity ($B < 0.4$). The linear relationships between T_w and T_a has a higher slope (B values) upstream and much lower slopes, typically near zero, at spring locations (Table S2). In general, T_a explained over 70% of the variability in T_w, although each location had a unique relationship.

The relationship ($T_w(T_s, T_a, R_s$ and $G_L)$) was used to develop four predictive models of T_w based on (1&2) linear regression with either T_a or T_s, (3) multiple linear regression (*mlr*), and (4) stepwise (*sw*) nonlinear models for all locations (Table 2). At hourly time steps, averaged over all instream locations, the $T_w(T_s)$ had a lower RMSE (1.2 °C) and higher R^2 (0.74) than $T_w(T_a)$, which was likely due to the reduced time offset in T_s. At daily times steps, combining T_a, T_s, and R_s into the *mlr* model resulted in a mean RMSE of < 1 °C for daily mean and minimum T_w. The RMSE for the daily maximum was slightly over 1 °C. The addition of downstream river stage (G_L) improved our model, reducing the RMSE by ~ 0.1 °C. The *sw* regression reduced the RMSE to 0.63 °C and increased R^2 of 0.91 for daily mean T_w; this was essentially the most parameterized model. Given the 0.5 °C accuracy of our temperature sensors, uncertainties in the predictions are acceptable but limited to calibration period. However, if a similar correspondence is found to longer duration measurements (e.g. NLDAS forcing data), we can significantly increase the time duration.

Table 2
Predictive model performance in root mean square error (RMSE) and coefficient of determination (R^2) for hourly and daily water temperatures (T_w) using observed and NLDAS prediction variables in linear, multi-linear (*mlr*) and stepwise (*sw*) models.

	Hourly T_w					
Predictor	RMSE [°C]	R^2				
T_a	1.50	0.68				
T_s	1.22	0.74				
	Daily mean T_w		Daily max T_w		Daily min T_w	
Predictor(s)	RMSE [°C]	R^2	RMSE [°C]	R^2	RMSE [°C]	R^2
T_a	1.01	0.78	1.47	0.69	0.98	0.79
T_s	0.98	0.79	1.23	0.74	0.98	0.79
mlr(T_s, T_a, R_s)	0.91	0.81	1.16	0.77	0.94	0.80
mlr(G_L, T_s, T_a, R_s)	0.84	0.83	1.04	0.80	0.89	0.81
sw(G_L, T_s, T_a, R_s)	0.63	0.91	0.75	0.88	0.75	0.88
	NLDAS mean T_w		NLDAS max T_w		NLDAS min T_w	
Predictor(s)	RMSE [°C]	R^2	RMSE [°C]	R^2	RMSE [°C]	R^2
T_a	0.97	0.79	1.40	0.70	1.01	0.78
T_s	0.86	0.81	1.14	0.76	1.04	0.78
mlr(T_s, T_a, R_s)	0.84	0.83	1.08	0.78	0.91	0.81

First, each NLDAS variable was aggregated to HUC_{12}, HUC_{10} and HUC_8 and compared against meteorological observations. Regardless of aggregation size, the NLDAS T_a corresponds well to measured T_a (Fig. 7a). The HUC_{12} daily mean T_a had an adjusted R^2 of 0.96, an RMSE of 1.57 °C, a slope of 0.95, and an intercept of −0.1 °C. For T_s, observations were consistently warmer (+4.6 °C), again regardless of HUC size (Fig. 7b). The daily mean R_s (Fig. 7c) from NLDAS was consistently higher (+1.6 MJ m^{-2} d^{-1}); however, the weather station was located on the valley bottom and likely shaded by the surrounding hills at low sun angles. At the ⅛° scale, the NLDAS R_s was less affected by topography and may represent the watershed better than the measured data.

Next, the predictor variables (e.g. T_a, T_s, R_s) from the weather station data was replaced with NLDAS aggregated HUC_{12} values and developed a new coefficient for Eqs. (2) and (3). Note, river stage at the lower gage (G_L) was not available over the long-term so it was omitted hereafter. The performance of each model is presented in Fig. S14. Like the results for measured data, the use of T_s had a lower RMSE than T_a; however, the *mlr* clearly outperformed both (Table 2) and appears robust over the ~1000 days. We present a summertime snapshot of 2017 modeled daily maximum T_w results using NLDAS T_a, T_s, and *mlr* models from the upstream to downstream locations in Fig. 8. All three models tend to capture the warming trend through July when a frontal pattern drops temperatures.

Given the prior assumptions, 30 years of T_w data was simulated for each instream location using the HUC_{12} *mlr* model driven by NLDAS forcing data and calculated the 7-day anomalies. The residuals of the

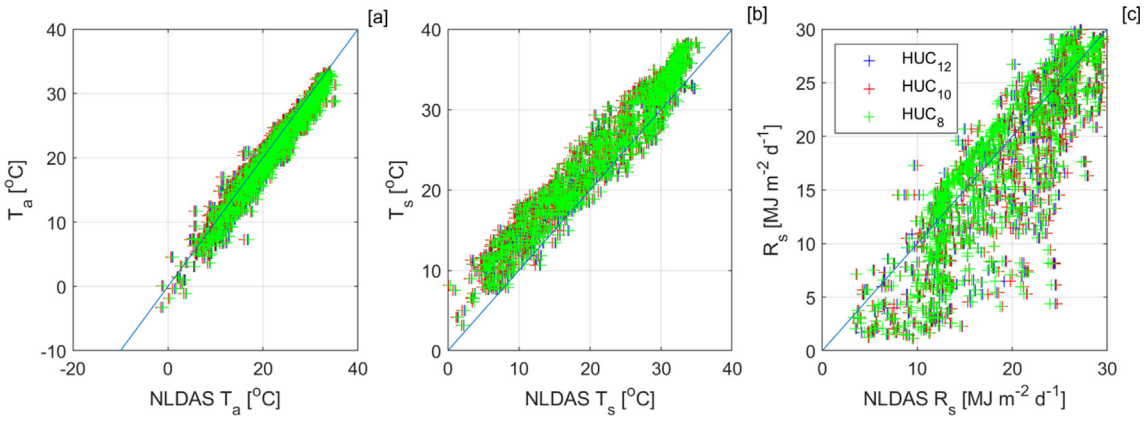

Fig. 7. Comparison between the NLDAS model aggregated to HUC_8, HUC_{10} and HUC_{12} scales and observed [a] hourly air temperature (T_a), [b] hourly soil temperature (T_s), and [c] daily accumulated solar radiation (R_s).

linear trend are normally distributed with a zero-mean, which improves the robustness of least-squares regression for trend detection. Both the daily maximum T_a and T_s increased by 0.35° and 0.30 °C per decade, respectively, over the HUC_{12} area (Fig. S15). Given that the models were explicitly based on these, it was not surprising that T_w also has an increasing trend over the past 30 years, particularly where thermal sensitivity (*B*) was greater. Assuming spring temperatures and discharge had remained consistent, instream locations with greater temperature sensitivity (e.g. higher *B*) will also have greater trends in T_w, as illustrated by the highest *B* (upstream) at 0.16 °C per decade (S15c) and a lower *B* from the downstream at 0.12 °C per decade.

All correlations to daily maximum T_a, T_s, and predicted T_w are

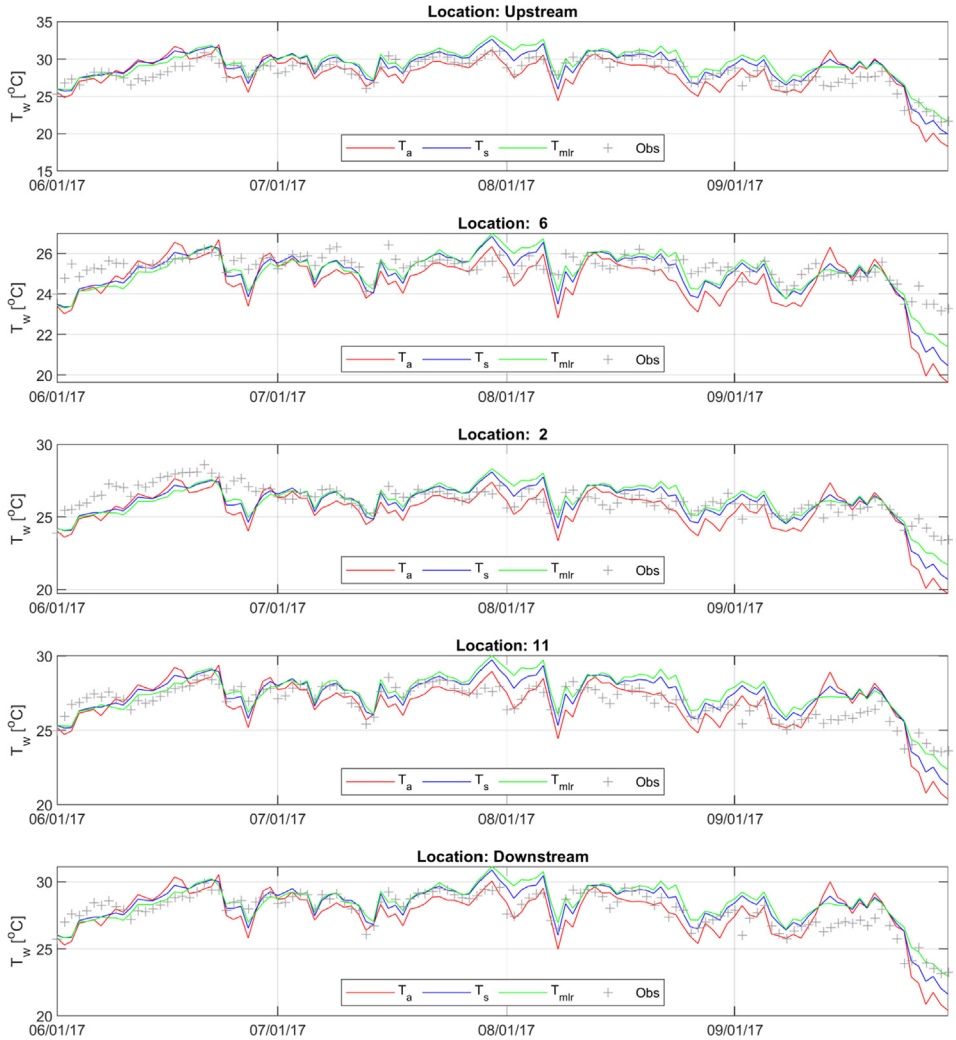

Fig. 8. Summer (2017) time series plot of modeled instream daily maximum temperatures (T_w) using NLDAS T_a, T_s, and T_{mlr} at select monitoring locations shown in Fig. 1.

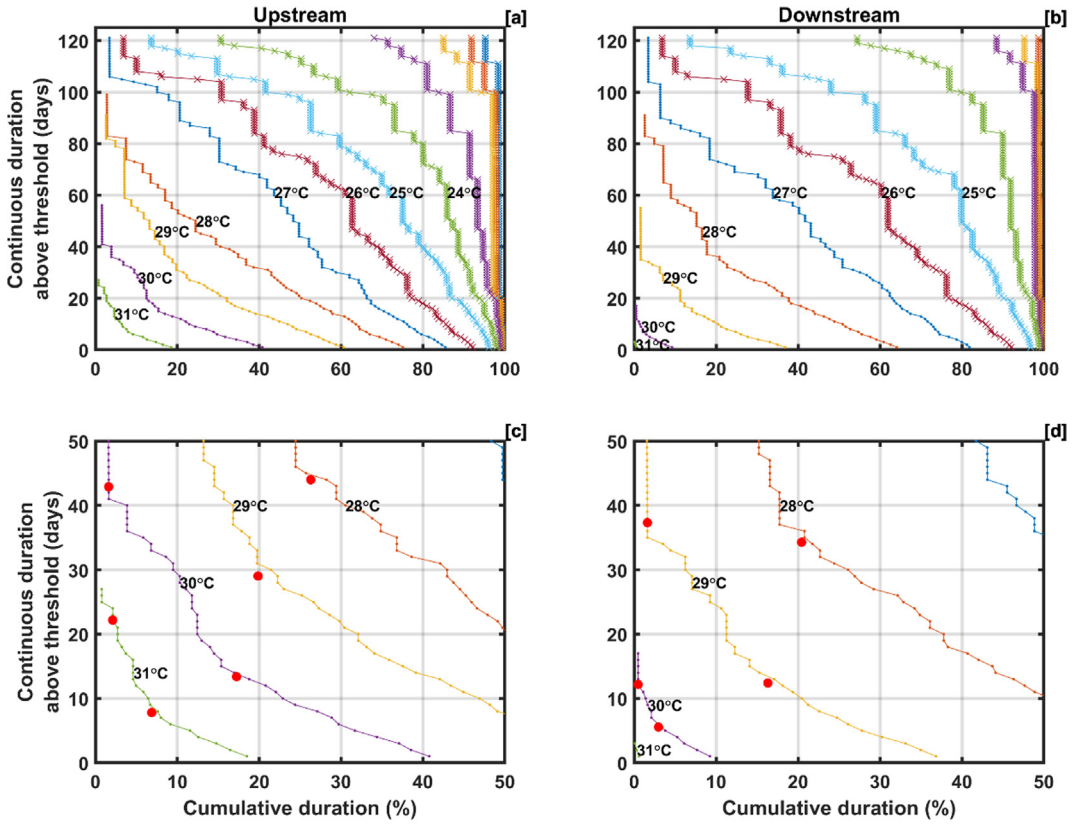

Fig. 9. The frequency and duration by uniform continuous above-threshold (UCAT) analysis of thermal events using data from 30-yr maximum daily T_w between June 1-Sept 30 at the [a] upstream and [b] downstream locations. The lower panel [c&d] are zoomed to indicate inflection points in each probability distribution.

significant ($p < 0.05$) based on either t-Test or Mann-Kendall trend test (Table S3). No significant trend was detected for daily minimum temperatures, and only daily mean T_a and #19 (Fig. 1) at the Dolan Creek outflow were significant based on Mann-Kendall tests. Given that the springs buffer this system from temperature extremes, any change to spring discharge could significantly amplify the climate change signal (0.35 °C per decade).

4.6. Thermal habitat thresholds

The magnitude, frequency, and duration of instream T_w was quantified using UCAT analysis that determined the cumulative time values of T_w exceeding an inflection threshold. The UCAT curves are essentially a three dimensional space of duration (x-axis), frequency (y-axis), and maximum daily T_w (z-axis) where common versus uncommon events are denoted by rapid changes in slope from 'persistent' to 'catastrophic' (Parasiewicz, 2008) (e.g., Fig. S10). The upstream location had higher summer temperatures than the downstream resulting from 44% of the downstream flow being derived from spring discharge. As an example, there was a 20% chance in the maximum T_w reaching 28 °C for 60 continuous days upstream (Fig. 9a) while only a 10% probability downstream (Fig. 9b) over the past 30 years. To evaluate persistent and catastrophic conditions, we focused on extreme temperatures and their inflections in the continuous duration curves, which mark periods of rapid departure (Castelli et al., 2012). For upstream (Fig. 9c), T_w at 30 °C was persistent for 13 days and catastrophic for 43 days while downstream (Fig. 9d) critical thresholds were 6 days and catastrophic at 12 days (Table S4). Thus, spring discharge reduced the time above these thresholds by 50 and 70%, respectively. Without direct measurements of species-dependent lethality from laboratory experiments or field data, these thresholds only provide reasonable criteria for management action.

5. Discussion

Discrete discharge from karst aquifers from springs maintains the thermal and hydrological regimes needed to support aquatic life in the Devils River. A strong thermal sensitivity of water temperatures to air was found, but an even stronger sensitivity to soil temperatures. Little research has shown such a connection. Burns et al. (2017) found that at the decadal scale land surface temperatures are translated to groundwater temperatures. The vulnerability of these species to changes in stream temperature is thus difficult to ascertain without long-term observations. Protection of GDE is hampered by a general lack of information on such systems (Howard and Merrifield, 2010) and acquiring such data was particularly challenging in the remote and harsh field site. A temporally sparse, yet spatially diverse T_w dataset from instream sensors and DTS-FO in various geomorphic positions along a karst spring complex was used to fill and extend our period of record using 30 years of climatic forcing data from NLDAS and then assess trends and the magnitude, frequency, and duration of UCAT thermal events. Even with decadal increases in air and soil temperatures, springs provide a consistent thermal buffer and heterogenous aquatic habitat.

Our analysis assumed consistent groundwater discharge over 30-years. We measured ~30 m of hydraulic head above these spring complexes, providing a stable hydrological regime for the GDE. However, the preferential flow paths through the carbonate aquifer system and rapid response to local recharge events suggest a system that is highly susceptible to perturbation from either drought or groundwater abstraction. (Green et al., 2014). Thus, impacts of climate change on instream temperatures may be significantly outweighed by reductions in discharge from groundwater abstraction that may alter the UCAT inflection thermal regime thresholds point obtained. Current research suggests chronic water temperatures over 27 °C may increase the mortality of the Devils River minnow with lethality likely near 30 °C

(Fries and Gibson, 2013).

Along the remote Devils River, neither land use nor riparian structure has changed significantly; however, environmental drivers, such as T_a and T_s were found to be increasing. Through the modeling, we estimate that daily maximum T_w has also increased at 0.01–0.16 °C per decade with higher rates in locations more sensitive to thermally driven heat advection. Cold-water fisheries, such as the lower Klamath River in southern Oregon and northern California, have seen a more dramatic temperature increases of 0.5 °C per decade (Bartholow, 2005). Groundwater discharge can be the dominant control on thermal refugia for the endangered dwarf wedgemussel (*Aslasmidonta heterodon*) of New England (Briggs et al., 2013). Recently, the Texas Hornshell (*Popenaias popeii*), which is a medium sized freshwater mussel endemic to the Rio Grande River and its tributaries, has been listed as endangered (USFWS, 2018) with only four populations remaining (Randklev et al., 2018b). Two Texas Hornshell mussel beds were identified within our study reach, both on discrete gravel beds in shallow riffles. One bed near the upstream location was subaerially exposed following the 2011 statewide drought which led to predation by raccoons (*Procyon lotor*). Morphologic channel features (i.e. pool, riffle, run) are important mesohabitats for endemic, threatened species (Robertson and Winemiller, 2003). Many arid fisheries are relict species, highly endemic, and threatened by human expansion into these unique habitats (Rolston, 1991). Refugia, both thermal and evolutionary, have been suggested as priority sites for conservation under climate change because of their ability to facilitate survival of biota under extreme conditions (Davis et al., 2013). Many fisheries are suffering from both anthropogenic changes to their habitats (i.e. dams, flood control, etc.) and increasing water temperatures resulting from changes to riparian structure and climate.

Thus, excessive groundwater withdrawals, drought, and climate change underscore the need for environmental flow standards to protect habitat for these species (Opdyke et al., 2014; Randklev et al., 2018a). Unionid mussels, such as the Texas Horshell, are sensitive to high water temperatures, especially during early life stages (Maloney et al., 2012). The Texas Hornshell evolved at the same time as *Dionda Diaboli* and the larger native fish communtiy. Thus, reduced spring discharge from either drought or groundwater extraction along with increasing instream water temperatures related to climate change could adversely affect thermal buffering and potentially eliminate aquatic habitats for these threatened and endangered species. While ongoing research seeks to understand thermal tolerances of *P. Popeii*, glochidia (freshwater mussel larvae) of Unionid species in central and east Texas streams have median lethal temperatures (LD50) of 26.9–36.4 °C and a mean of 32.4 °C (Khan et al., 2019). The extent of the economic impact of maintaining a healthy aquatic ecosystem for mussels and any other species of conservation interest would depend on the implementation of water laws, which could regulate groundwater pumping to maintain environmental flows, particularly given the aridity and karstic nature of the Devils River watershed (Wolaver et al., 2014). There is a paucity of studies on environmental flows and GDE in arid lands and many significant gaps in basic data collection (Mott Lacroix et al., 2017).

The springs and caves associated GDE in karst aquifers are hotspots of biodiversity (Goldscheider, 2019). A synergistic hydrogeologic and ecologic approach is needed to derive the basic operations of these GDE in order to understand their future trajectory (Cantonati et al., 2020). Future research should assess climate projections on the thermal regimes in the Devils River watershed and how it may impact environmental flows. The shallow monitoring well is too close to springs to make an effective “sentinel” well per Harrington and Rainville (2017). We anticipate expanding the well monitoring network upgradient of the GDE. Ideally, collection of hydrogeologic data over a larger area may allow a possible “trigger well” further afield from the study area at which regional scale fluctuations in groundwater levels are well correlated with longer-term spring discharge trends. In addition, an airborne Light Detection and Ranging (Lidar) bathymetric and topographic survey data were acquired in March 2018 along the Devils River from Lake Amistad to its headwaters ~70 km upstream near Juno, Texas. The bathymetric and topographic Lidar elevation models will provide input to aquatic habitat models used to assess habitat suitability for a suite of aquatic species (including *D. diaboli* and *P. popeii*) under a range of instream flow scenarios and be used to classify stream mesohabitats and map aquatic vegetation. Ultimately, the physical habitat model could be used in conjunction with a groundwater model to understand how instream flows may change in response to groundwater development scenarios in the basin. While this approach was applied to aquatic habitats in the Devils River of Texas, this research approach may be used to inform conservation in other semi-arid, highly groundwater dependent streams with important species of state and federal conservation interest.

6. Conclusions

The 3-year monitoring shows that stable discharge from the spring complex provided ~40% of downstream discharge in the Devils River and buffered river temperatures by ~50%. By correlating short-term monitoring data with modeled long-term temperature data, the surface water temperature records were extended to 30 years, revealing a long-term warming trend with daily maximum water temperature increasing 0.16 °C per decade. Model-derived daily maximum air temperature also increased by 0.35 °C per decade. Our uniform continuous above threshold analysis shows that the consistent spring temperatures of 22.6 ± 0.3 °C reduced the duration of above 30 °C temperature days by 50–70% downstream of the spring complex. This long-term air and water temperature evaluation suggests susceptibility to climate change; however, extreme drought and groundwater depletion represent more acute problems in the near-term for such karst environments. Given the lack of regulations to protect groundwater, unsustainable groundwater development poses a particular threat to spring discharge. This study underscores the need for developing a suitable monitoring program with basin-wide sentinel groundwater wells and establish threshold groundwater pumping levels to maintain spring flows and temperatures needed to preserve aquatic habitats for protected species. To this end ongoing development of groundwater and surface water models will inform this process. Although the approach developed in this study was applied to the Devils River of Texas, the techniques could be widely applied to GDE in similar regions globally. The monitoring and modeling analysis provide the science needed to understand the aquifer-spring-stream interconnections to manage groundwater development at a level that maintains spring discharge and buffer temperatures in aquatic habitats of conservation interest.

CRediT authorship contribution statement

Todd G. Caldwell: Conceptualization, Methodology, Formal analysis, Writing - original draft, Writing - review & editing, Visualization. **Brad D. Wolaver:** Conceptualization, Methodology, Writing - original draft, Writing - review & editing. **Tara Bongiovanni:** Formal analysis, Investigation, Data curation, Writing - review & editing, Visualization. **Jon P. Pierre:** Investigation, Data curation, Writing - review & editing, Visualization. **Sarah Robertson:** Validation, Resources, Funding acquisition. **Charles Abolt:** Investigation, Writing - review & editing. **Bridget R. Scanlon:** Validation, Resources, Writing - review & editing.

Declaration of Competing Interest

The authors declare that they have no known competing financial interests or personal relationships that could have appeared to influence the work reported in this paper.

Acknowledgments

Support for this study was provided by the U.S. Fish and Wildlife Service and the Texas Parks and Wildlife Department, Section 6 Grant #TX E-173-R-1, F15AP00669 and State and Tribal Wildlife Grant #507663. All time series data collected during this study and referenced to Fig. 1 will be made available for download online and at https://doi.org/10.18738/T8/MGNNQV. Thanks to K. Mayes, K. Aziz, C. Robertson, and S. Magnelia (TPWD); R. Smith (TNC); L. French and A. Weinberg (TWDB) for helpful discussions and technical support; J. Joplin, B. Hester, W. Collins, (TPWD) at the Devils River SNA; H. Pai, S. Tyler, S. Sladek, and C. Kratt (CTEMPS) for UAV/DTS support; M. Hausner (DRI) and B. Cardenas (UT-DGS) for the DTS system; J. Andrews, J. Hupp, K. Salyam, A. Averett, and C. Breton (UT-BEG) for help with data collection, processing, and mapping; K. Allander (USGS) for editorial review; M. Montagne, P. Diaz, and R. Gibson (FWS) for support; D. Hester, R. Smith, and D. Meyer (TNC) for logistics while at the Dolan Falls Preserve.

Appendix A. Supplementary data

Supplementary data to this article can be found online at https://doi.org/10.1016/j.jhydrol.2020.124947.

References

Abbott, P.L., 1975. On the hydrology of the edwards limestone, south-central Texas. J. Hydrol. 24, 251–269.

Abolt, C., Caldwell, T., Wolaver, B., Pai, H., 2018. Unmanned aerial vehicle-based monitoring of groundwater inputs to surface waters using an economical thermal infrared camera. Opt. Eng. 57 (9), 053113. https://doi.org/10.1117/1.Oe.57.5.053113.

Acreman, M., Dunbar, M.J., 2004. Defining environmental river flow requirements - a review. Hydrol. Earth Syst. Sci. 8, 861–876.

Albertson, L.K., Ouellet, V., Daniels, M.D., 2018. Impacts of stream riparian buffer land use on water temperature and food availability for fish. J. Freshw. Ecol. 33, 195–210. https://doi.org/10.1080/02705060.2017.1422558.

Allan, J.D., Castillo, M.M., 2007. Stream Ecology: Structure and Function of Running Waters 436, pp.,.Stream Ecology : Structure and Function of Running Waters, second ed. Springer, Dondrecht, The Netherlands, pp. 436.

Anderson, M.P., 2005. Heat as a ground water tracer. Ground Water 43, 951–968.

Atkinson, D. (1994), Temperature and organism size — a biological law for ectotherms, in Advances in Ecological Research, Vol 25, edited by M. Begon and A. H. Fitter, pp. 1-58.

Barker, R. A., P. W. Bush, and E. T. Baker (1994), Geologic history and hydrogeologic setting of the Edwards-Trinity aquifer system, west-central Texas, U.S. Geological Survey, Water-Resources Investigations Report 94-4039, 51 pp, Austin, TX.

Bartholow, J. M. (2005), Recent water temperature trends in the lower Klamath River, California, North American Journal of Fisheries Management, 25, 152-162.

Beaufort, A., Moatar, F., Sauquet, E., Loicq, P., Hannah, D.M., 2019. Influence of landscape and hydrological factors on stream-air temperature relationships at regional scale. Hydrol. Process. https://doi.org/10.1002/hyp.13608, 1-19, 10.1002/hyp.13608.

Briggs, M.A., Hare, D.K., 2018. Explicit consideration of preferential groundwater discharges as surface water ecosystem control points. Hydrol. Process. 32, 2435–2440. https://doi.org/10.1002/hyp.13178.

Briggs, M.A., Lautz, L.K., McKenzie, J.M., 2012. A comparison of fibre-optic distributed temperature sensing to traditional methods of evaluating groundwater inflow to streams. Hydrol. Process. 26, 1277–1290.

Briggs, M.A., Voytek, E.B., Day-Lewis, F.D., Rosenberry, D.O., Lane, J.W., 2013. Understanding water column and streambed thermal refugia for endangered mussels in the Delaware River. Environ. Sci. Technol. 47, 11423–11431.

Brown, J., Bach, L., Aldous, A., Wyers, A., DeGagne, J., 2011. Groundwater-dependent ecosystems in Oregon: an assessment of their distribution and associated threats. Front. Ecol. Environ. 9, 97–102. https://doi.org/10.1890/090108.

Burns, E.R., Zhu, Y.H., Zhan, H.B., Manga, M., Williams, C.F., Ingebritsen, S.E., Dunham, J.B., 2017. Thermal effect of climate change on groundwater-fed ecosystems. Water Resour. Res. 53, 3341–3351. https://doi.org/10.1002/2016wr020007.

Burt, T.P., McDonnell, J.J., 2015. Whither field hydrology? The need for discovery science and outrageous hydrological hypotheses. Water Resour. Res. 51, 5919–5928. https://doi.org/10.1002/2014wr016839.

Cantonati, M., Stevens, L.E., Segadelli, S., Springer, A.E., Goldscheider, N., Celico, F., Filippini, M., Ogata, K., Gargini, A., 2020. Ecohydrogeology: the interdisciplinary convergence needed to improve the study and stewardship of springs and other groundwater-dependent habitats, biota, and ecosystems. Ecol. Ind. 110, 105803. https://doi.org/10.1016/j.ecolind.2019.105803.

Capra, H., Breil, P., Souchon, Y., 1995. A new tool to interpret magnitude and duration of fish habitat variations. Regul. Rivers-Res. Manage. 10, 281–289.

Castelli, E., Parasiewicz, P., Rogers, J.N., 2012. Use of frequency and duration analysis for the determination of thermal habitat thresholds: application for the conservation of *Alasmidonta heterodon* in the Delaware River. J. Environ. Eng. 138, 886–892.

Chung, K.S., 2001. Critical thermal maxima and acclimation rate of the tropical guppy *Poecilla reticulata*. Hydrobiologia 462, 253–257.

Colinet, H., Sinclair, B.J., Vernon, P., Renault, D., 2015. Insects in fluctuating thermal environments. Annu. Rev. Entomol. 60, 123–140. https://doi.org/10.1146/annurev-ento-010814-021017.

Constantz, J., 1998. Interaction between stream temperature, streamflow, and groundwater exchanges in Alpine streams. Water Resour. Res. 34, 1609–1615.

Constantz, J., Naranjo, R., Niswonger, R., Allander, K., Neilson, B., Rosenberry, D., Smith, D., Rosecrans, C., Stonestrom, D., 2016. Groundwater exchanges near a channelized versus unmodified stream mouth discharging to a subalpine lake. Water Resour. Res. 52, 2157–2177. https://doi.org/10.1002/2015wr017013.

Craig, C.A., Kollaus, K.A., Behen, K.P.K., Bonner, T.H., 2016. Relationships among spring flow, habitats, and fishes within evolutionary refugia of the Edwards Plateau. Ecosphere 7, E01205. https://doi.org/10.1002/ecs2.1205.

Davis, J., Pavlova, A., Thompson, R., Sunnucks, P., 2013. Evolutionary refugia and ecological refuges: key concepts for conserving Australian arid zone freshwater biodiversity under climate change. Glob. Change Biol. 19, 1970–1984. https://doi.org/10.1111/gcb.12203.

Dzara, J.R., Neilson, B.T., Null, S.E., 2019. Quantifying thermal refugia connectivity by combining temperature modeling, distributed temperature sensing, and thermal infrared imaging. Hydrol. Earth Syst. Sci. 23, 2965–2982. https://doi.org/10.5194/hess-23-2965-2019.

El-Hage, A., and D. W. Moulton (2001), Ecologically significant river and stream segments of Region J (Plateau), regional water planning area: Devils River, Texas Parks and Wildlife Department, 45-47 pp, Austin, TX.

Fries, J.N., Gibson, R., 2013. Effects of temperature on captive-bred Devils River minnows. Southwestern Natur. 58, 330–334. https://doi.org/10.1894/0038-4909-58.3.330.

Goldscheider, N., 2019. A holistic approach to groundwater protection and ecosystem services in karst terrains. Carbonates Evaporites 34, 1241–1249. https://doi.org/10.1007/s13146-019-00492-5.

Green, R.T., Bertetti, F.P., Miller, M.S., 2014. Focused groundwater flow in a carbonate aquifer in a semi-arid environment. J. Hydrol. 517, 284–297.

Hardy, T.B., 1998. The future of habitat modeling and instream flow assessment techniques. Regul. Rivers-Res. Manage. 14, 405–420.

Hare, D.K., Briggs, M.A., Rosenberry, D.O., Boutt, D.F., Lane, J.W., 2015. A comparison of thermal infrared to fiber-optic distributed temperature sensing for evaluation of groundwater discharge to surface water. J. Hydrol. 530, 153–166.

Harrington, R., K. Rainville, and T. N. Blandford (2017), Comment on “Drawdown 'Triggers': a misguided strategy for protecting groundwater-fed streams and springs,” by Matthew J. Currell, 2016, v. 54, no. 5: 619-622, Groundwater, 55, 152-153, 10.1111/gwat.12503.

Hausner, M.B., Wilson, K.P., Gaines, D.B., Tyler, S.W., 2012. Interpreting seasonal convective mixing in Devils Hole, Death Valley National Park, from temperature profiles observed by fiber-optic distributed temperature sensing. Water Resour. Res. 48, W05513. https://doi.org/10.1029/2011wr010972.

Hausner, M.B., Wilson, K.P., Gaines, D.B., Suarez, F., Scoppettone, G.G., Tyler, S.W., 2016. Projecting the effects of climate change and water management on Devils Hole pupfish (*Cyprinodon diabolis*) survival. Ecohydrology 9, 560–573. https://doi.org/10.1002/eco.1656.

Howard, J., Merrifield, M., 2010. Mapping groundwater dependent ecosystems in California. PLoS ONE 5, e11249. https://doi.org/10.1371/journal.pone.0011249.

Hubbs, C., 1995. Springs and spring runs as unique aquatic systems. Copeia 4, 989–991. https://doi.org/10.2307/1447053.

Hubbs, C., Brown, W.H., 1956. *Dionda diaboli* (Cyprinidae), a new minnow from Texas. Southwest Natur. 1, 69–77.

Huntington, J., McGwire, K., Morton, C., Snyder, K., Peterson, S., Erickson, T., Niswonger, R., Carroll, R., Smith, G., Allen, R., 2016. Assessing the role of climate and resource management on groundwater dependent ecosystem changes in arid environments with the Landsat archive. Remote Sens. Environ. 185, 186–197. https://doi.org/10.1016/j.rse.2016.07.004.

Isaak, D. J., D. L. Horan, and S. P. Wollrab (2013), A simple protocol using underwater epoxy to install annual temperature monitoring sites in rivers and streams, U.S. Department of Agriculture, Forest Service, Rocky Mountain Research Station, RMRS-GTR-314, 21 pp, Fort Collins, CO.

Johnson, A.N., Boer, B.R., Woessner, W.W., Stanford, J.A., Poole, G.C., Thomas, S.A., O'Daniel, S.J., 2005. Evaluation of an inexpensive small-diameter temperature logger for documenting ground water-river interactions. Ground Water Monit. Rem. 25, 68–74. https://doi.org/10.1111/j.1745-6592.2005.00049.x.

Kaandorp, V.P., Doornenbal, P.J., Kooi, H., Peter Broers, H., de Louw, P.G.B., 2019. Temperature buffering by groundwater in ecologically valuable lowland streams under current and future climate conditions. J. Hydrol. X 3, 100031. https://doi.org/10.1016/j.hydroa.2019.100031.

Kamps, R.H., Tatum, G.S., Gault, M., Groeger, A.W., 2009. Goodenough Spring, Texas, USA: discharge and water chemistry of a large spring deeply submerged under the binational Amistad Reservoir. Hydrogeol. J. 17, 891–899. https://doi.org/10.1007/s10040-008-0404-0.

Kelleher, C., Wagener, T., Gooseff, M., McGlynn, B., McGuire, K., Marshall, L., 2012. Investigating controls on the thermal sensitivity of Pennsylvania streams. Hydrol. Process. 26, 771–785. https://doi.org/10.1002/hyp.8186.

Khan, J.M., Hart, M., Dudding, J., Robertson, C.R., Lopez, R., Randklev, C.R., 2019. Evaluating the upper thermal limits of glochidia for selected freshwater mussel species (Bivalvia: Unionidae) in central and east Texas, and the implications for their

conservation. Aquat. Conserv. Mar. Freshw. Ecosyst. 29, 1202–1215. https://doi.org/10.1002/aqc.3136.
Kochel, R.C., Baker, V.R., Patton, P.C., 1982. Paleohydrology of southwestern Texas. Water Resour. Res. 18, 1165–1183.
Kollaus, K.A., Bonner, T.H., 2012. Habitat associations of a semi-arid fish community in a karst spring-fed stream. J. Arid Environ. 76, 72–79.
Kurylyk, B.L., MacQuarrie, K.T.B., Voss, C.I., 2014. Climate change impacts on the temperature and magnitude of groundwater discharge from shallow, unconfined aquifers. Water Resour. Res. 50, 3253–3274. https://doi.org/10.1002/2013wr014588.
Maloney, K.O., Lellis, W.A., Bennett, R.M., Waddle, T.J., 2012. Habitat persistence for sedentary organisms in managed rivers: the case for the federally endangered dwarf wedgemussel (*Alasmidonta heterodon*) in the Delaware River. Freshw. Biol. 57, 1315–1327. https://doi.org/10.1111/j.1365-2427.2012.02788.x.
Mitchell, K.E., Lohmann, D., Houser, P.R., Wood, E.F., Schaake, J.C., Robock, A., Cosgrove, B.A., Sheffield, J., Duan, Q.Y., Luo, L.F., Higgins, R.W., Pinker, R.T., Tarpley, J.D., Lettenmaier, D.P., Marshall, C.H., Entin, J.K., Pan, M., Shi, W., Koren, V., Meng, J., Ramsay, B.H., Bailey, A.A., 2004. The multi-institution north american land data assimilation system (NLDAS): utilizing multiple GCIP products and partners in a continental distributed hydrological modeling system. J. Geophys. Res. Atmos. 109, D07S90. https://doi.org/10.1029/2003jd003823.
Mohseni, O., Stefan, H.G., 1999. Stream temperature air temperature relationship: a physical interpretation. J. Hydrol. 218, 128–141.
Mott Lacroix, K.E., Tapia, E., Springer, A., 2017. Environmental flows in the desert rivers of the United States and Mexico: synthesis of available data and gap analysis. J. Arid Environ. 140, 67–78.
MRLC (2018), Multi-Resolution Land Characteristics Consortium, National Land Cover Database (NLCD), accessed 13 August 2018, http://www.mrlc.gov.
Mundy, E., Gleeson, T., Roberts, M., Baraer, M., McKenzie, J.M., 2017. Thermal imagery of groundwater seeps: possibilities and limitations. Groundwater 55, 160–170.
National Research Council, 2005. The Science of Instream Flows: A Review of the Texas Instream Flow Program. The National Academies Press, Washington, D.C, doi.org/10.17226/11197.
Opdyke, D.R., Oborny, E.L., Vaugh, S.K., Mayes, K.B., 2014. Texas environmental flow standards and the hydrology-based environmental flow regime methodology. Hydrol. Sci. J. Des Sci. Hydrol. 59, 820–830. https://doi.org/10.1080/02626667.2014.892600.
Pai, H., Malenda, H.F., Briggs, M.A., Singha, K., Gonzalez-Pinzon, R., Gooseff, M.N., Tyler, S.W., AirCTEMPS Team, 2017. Potential for small unmanned aircraft systems applications for identifying groundwater-surface water exchange in a meandering river reach. Geophys. Res. Lett. 44, 11868–11877. https://doi.org/10.1002/2017GL075836.
Parasiewicz, P., 2008. Habitat time series analysis to define flow augmentation strategy for the Quinebaug River Connecticut and Massachusetts, USA. River Res. Appl. 24, 439–452.
Poff, N.L., Allan, J.D., 1995. Functional-organization of stream fish assemblages in relation to hydrological variability. Ecology 76, 606–627. https://doi.org/10.2307/1941217.
Poole, G.C., Berman, C.H., 2001. An ecological perspective on in-stream temperature: natural heat dynamics and mechanisms of human-caused thermal degradation. Environ. Manage. 27, 787–802. https://doi.org/10.1007/s002670010188.
Power, G., Brown, R.S., Imhof, J.G., 1999. Groundwater and fish - insights from northern North America. Hydrol. Process. 13, 401–422.
PRISM (2018), Oregon State Univeristy, accessed 13 August 2018, http://prism.oregonstate.edu.
Randklev, Charles R., Tsakris, Eric T., Johnson, Matthew S., Popejoy, Traci, Hart, Michael A., Khan, Jennifer, Geeslin, Dakus, Robertson, Clinton R., 2018a. The effect of dewatering on freshwater mussel (Unionidae) community structure and the implications for conservation and water policy: a case study from a spring-fed stream in the southwestern United States. Global Ecol. Conserv. 16, e00456. https://doi.org/10.1016/j.gecco.2018.e00456.
Randklev, C.R., Miller, T., Hart, M., Morton, J., Johnson, N.A., Skow, K., Inoue, K., Tsakiris, E.T., Oetker, S., Smith, R., Robertson, C., Lopez, R., 2018b. A semi-arid river in distress: Contributing factors and recovery solutions for three imperiled freshwater mussels (Family Unionidae) endemic to the Rio Grande basin in North America. Sci. Total Environ. 631–632, 733–744. https://doi.org/10.1016/j.scitotenv.2018.03.032.
Rantz, S. E. (1982), Measurement and computation of streamflow: Volume 2, Computation of Discharge, U.S. Geological Survey, Water-Supply Paper 2175, 285-631 pp.
Robertson, M.S., Winemiller, K.O., 2003. Habitat associations of fishes in the Devils River Texas. J. Freshw. Ecol. 18, 115–127.
Robertson, S., B. Wolaver, T. G. Caldwell, T. Birdson, R. Smith, T. Hardy, J. Lewey, and J. Joplin (2019a), A multidisciplinary approach to developing the science and public support needed to maintain instream flows in the Devils River Basin, Texas, in Multispecies and Watershed Approaches to Freshwater Fish Conservation, edited by D. C. Dauwalter, T. Birdson and G. P. Garret, pp. 293–314, American Fisheries Society Symposia 91, Bethesda, MD.
Robertson, W.M., Allen, J.T., Wolaver, B.D., Sharp, J.M., 2019b. Aridland spring response to mesoscale precipitation: implications for groundwater-dependent ecosystem sustainability. J. Hydrol. 570, 850–862. https://doi.org/10.1016/j.jhydrol.2018.12.074.
Rohde, M.M., Froend, R., Howard, J., 2017. A global synthesis of managing groundwater dependent ecosystems under sustainable groundwater policy. Groundwater 55, 293–301. https://doi.org/10.1111/gwat.12511.
Rolston, H., 1991. Fishes in the desert: paradox and responsibility. In: Minckley, W.L., Decon, J.E. (Eds.), Battle Against Extinction: Native Fish Management in the American West. University of Arizona Press, Tucson, AZ, pp. 93–108.
Selker, J.S., Thevenaz, L., Huwald, H., Mallet, A., Luxemburg, W., de Giesen, N.V., Stejskal, M., Zeman, J., Westhoff, M., Parlange, M.B., 2006. Distributed fiber-optic temperature sensing for hydrologic systems. Water Resour. Res. 42, W12202. https://doi.org/10.1029/2006WR005326.
Snyder, C.D., Hitt, N.P., Young, J.A., 2015. Accounting for groundwater in stream fish thermal habitat responses to climate change. Ecol. Appl. 25, 1397–1419.
Springer, A.E., Stevens, L.E., 2009. Spheres of discharge of springs. Hydrogeol. J. 17, 83–93.
Stefan, H.G., Preudhomme, E.B., 1993. Stream temperature estimation from air temperature. Water Resour. Bull. 29, 27–45.
TWPD, 2012. Texas Conservation Action Plan 2012–2016: Statewide/Multi-region Handbook, Texas Parks and Wildlife Division, 78 pp. Austin, TX.
USFWS (2005), Devils River Minnow (Dionda diaboli) Recovery Plan, U.S. Fish and Wildlife Service, 123 pp, Albuquerque, NM.
USFWS, 2018. Endangered and threatened wildlife and plants; Endangered species status for Texas hornshell., U.S. Fish and Wildlife Service. Fed. Reg. 83 (28), 5720–5735.
van de Giesen, N., Steele-Dunne, S.C., Jansen, J., Hoes, O., Hausner, M.B., Tyler, S., Selker, J., 2012. Double-ended calibration of fiber-optic Raman spectra distributed temperature sensing data. Sensors 12, 5471–5485.
Wagner, R.J., Boulger, R.W., Oblinger, C.J., Smith, B.A., 2006. Guidelines and standard procedures for continuous water-quality monitors: station operation, record computation, and data reporting U.S. Geological Survey. Tech. Methods 1–D3, 51 pp.
Webb, B.W., Zhang, Y., 1997. Spatial and seasonal variability in the components of the river heat budget. Hydrol. Process. 11, 79–101.
Wolaver, B.D., Cook, C.E., Sunding, D.L., Hamilton, S.F., Scanlon, B.R., Young, M.H., Xu, X.L., Reedy, R.C., 2014. Potential economic impacts of environmental flows following a possible listing of endangered Texas freshwater mussels. J. Am. Water Resour. Assoc. 50, 1081–1101. https://doi.org/10.1111/jawr.12171.
Wondzell, S.M., Diabat, M., Haggerty, R., 2019. What matters most: are future stream temperatures more sensitive to changing air temperatures, discharge, or riparian vegetation? J. Am. Water Resour. Assoc. 55, 116–132. https://doi.org/10.1111/1752-1688.12707.
Xia, Y.L., Mitchell, K., Ek, M., Sheffield, J., Cosgrove, B., Wood, E., Luo, L.F., Alonge, C., Wei, H.L., Meng, J., Livneh, B., Lettenmaier, D., Koren, V., Duan, Q.Y., Mo, K., Fan, Y., Mocko, D., 2012. Continental-scale water and energy flux analysis and validation for the North American Land Data Assimilation System project phase 2 (NLDAS-2): 1 Intercomparison and application of model products. J. Geophys. Res. Atmos. 117, D03109. https://doi.org/10.1029/2011jd016048.